

DRAFT VERSION NOVEMBER 24, 2015
Preprint typeset using L^AT_EX style emulateapj v. 5/2/11

A DARK SPOT ON A MASSIVE WHITE DWARF*

MUKREMIN KILIC¹, ALEXANDROS GIANNINAS¹, KEATON J. BELL², BRANDON CURD¹, WARREN R. BROWN³, J. J. HERMES⁴,
PATRICK DUFOUR⁵, JOHN P. WISNIEWSKI¹, D. E. WINGET², K. I. WINGET²

Draft version November 24, 2015

ABSTRACT

We present the serendipitous discovery of eclipse-like events around the massive white dwarf SDSS J152934.98+292801.9 (hereafter J1529+2928). We selected J1529+2928 for time-series photometry based on its spectroscopic temperature and surface gravity, which place it near the ZZ Ceti instability strip. Instead of pulsations, we detect photometric dips from this white dwarf every 38 minutes. Follow-up optical spectroscopy observations with Gemini reveal no significant radial velocity variations, ruling out stellar and brown dwarf companions. A disintegrating planet around this white dwarf cannot explain the observed light curves in different filters. Given the short period, the source of the photometric dips must be a dark spot that comes into view every 38 min due to the rotation of the white dwarf. Our optical spectroscopy does not show any evidence of Zeeman splitting of the Balmer lines, limiting the magnetic field strength to $B < 70$ kG. Since up to 15% of white dwarfs display kG magnetic fields, such eclipse-like events should be common around white dwarfs. We discuss the potential implications of this discovery on transient surveys targeting white dwarfs, like the K2 mission and the Large Synoptic Survey Telescope.

Subject headings: starspots – white dwarfs

1. INTRODUCTION

White dwarfs are commonly used as spectrophotometric standards since the majority of them do not show any significant variations. The first pulsating white dwarf was in fact discovered by Landolt (1968) as part of his survey for new standard stars. Since then > 200 other DAV, DBV, and PG 1159 type variable white dwarfs have been identified in a variety of surveys (e.g., Mukadam et al. 2004).

Other sources of variability for white dwarfs include the relativistic beaming effect (Loeb & Gaudi 2003; Zucker et al. 2007), ellipsoidal variations, and eclipses. However, there are only a handful of white dwarfs known to display these effects (Shporer et al. 2010; Kilic et al. 2011; Parsons et al. 2013; Hermes et al. 2014; Hallakoun et al. 2015, and references therein). Eclipses can be due to (sub)stellar or planetary companions, and

Vanderburg et al. (2015) present the first candidate for a disintegrating planet around a white dwarf in the K2 mission data.

An alternate source of an ‘eclipse-like’ event on a white dwarf is a dark spot, or a starspot. There are several examples of white dwarfs with strong (> 1 MG) magnetic fields that display starspots, but a strong magnetic field is not always required or observed (Wickramasinghe & Ferrario 2000). RE J0317-853 belongs to the former category, where a $B = 340\text{--}450$ MG field is detected along with 0.2 mag peak-to-peak photometric variations due to a starspot that comes into view every 725 s due to the rotation of the white dwarf (Barstow et al. 1995; Ferrario et al. 1997). Gary et al. (2013) find 2.7 h period, low-amplitude (5 mma) optical variations on WD 2359-434, a magnetic white dwarf with a relatively low field strength of $B = 3.1 \pm 0.4$ kG (Aznar Cuadrado et al. 2004). GD 394 presents an unusual case where Dupuis et al. (2000) detect 25% amplitude variations in the extreme ultraviolet with a period of 1.15 d, but there is no evidence of a magnetic field down to a limit of 12 kG. Dupuis et al. (2000) interpret the observed photometric variations as evidence of surface abundance inhomogeneities.

The Kepler mission and the ongoing K2 mission are revealing that a large fraction of white dwarfs are variable. In addition to BOKS 53856, a magnetic white dwarf that displays 4.9% amplitude variations every 6.1 h (Holberg & Howell 2011), Maoz et al. (2015) find low-amplitude (60-2000 ppm) variations in half of the 14 white dwarfs observed as part of the original Kepler mission. This is unprecedented, as it implies that a large fraction of white dwarfs do indeed vary on hour-to-day timescales. The K2 mission has already discovered a disintegrating planet and a double white dwarf system in the first field (Vanderburg et al. 2015; Hallakoun et al. 2015), and a significant fraction of the K2 white dwarfs

* This work is based on observations obtained at the Gemini Observatory, McDonald Observatory, and the Apache Point Observatory 3.5-meter telescope. The latter is owned and operated by the Astrophysical Research Consortium. Gemini Observatory is operated by the Association of Universities for Research in Astronomy, Inc., under a cooperative agreement with the NSF on behalf of the Gemini partnership: the National Science Foundation (United States), the National Research Council (Canada), CONICYT (Chile), the Australian Research Council (Australia), Ministério da Ciência, Tecnologia e Inovação (Brazil) and Ministerio de Ciencia, Tecnología e Innovación Productiva (Argentina).

¹Homer L. Dodge Department of Physics and Astronomy, University of Oklahoma, 440 W. Brooks St., Norman, OK, 73019, USA

²Department of Astronomy, University of Texas at Austin, Austin, TX 78712, USA

³Smithsonian Astrophysical Observatory, 60 Garden St., Cambridge, MA 02138, USA

⁴Department of Physics, University of Warwick, Coventry CV4 7AL, UK

⁵Institut de recherche sur les exoplanètes (iREx), Département de Physique, Université de Montréal, C.P. 6128, Succ. Centre-Ville, Montréal, Québec H3C 3J7, Canada

do also show low-amplitude variations (N. Hallakoun 2015, private communication). Understanding the source of these variations is essential for transient surveys that are targeting large numbers of white dwarfs.

Here we present the serendipitous discovery of 38 min period optical photometric variations in an isolated massive white dwarf. Section 2 describes our target selection and follow-up observations, whereas Section 3 presents the results from our photometric and spectroscopic analysis. Section 4 visits three potential explanations for the observed photometric dips and demonstrates that a dark spot is the most likely source. We discuss the potential implications of this discovery on the K2 mission and the LSST, and conclude in Section 5.

2. TARGET SELECTION AND OBSERVATIONS

2.1. J1529+2928

We chose J1529+2928 for follow-up time-series photometry based on its temperature and surface gravity measurements from its Sloan Digital Sky Survey (SDSS) spectrum. Kleinman et al. (2013) classify it as a potentially magnetic DAH white dwarf based on this spectrum. However, there is no evidence of Zeeman splitting of the Balmer lines in our higher quality Gemini data (see below). Using the 1D atmosphere models for non-magnetic DA white dwarfs and the fitting procedures outlined in Gianninas et al. (2011), we find $T_{\text{eff}} = 11450$ K and $\log g = 8.88$ based on the SDSS data. These place J1529+2928 near the empirical boundaries of the ZZ Ceti instability strip (Gianninas et al. 2011). J1529+2928 is slightly cooler than the massive pulsating white dwarf BPM 37093, which has $T_{\text{eff}} = 11920 \pm 190$ K, $\log g = 8.81 \pm 0.05$, and pulsation periods between 512 and 635 s (Metcalfe et al. 2004).

2.2. Time-Series Photometry

We acquired high speed photometry of J1529+2928 using the Apache Point Observatory 3.5m Telescope with the Agile frame-transfer camera. We obtained 45 s long exposures with the BG40 filter over 1.7 h on UT 2015 April 10. We also obtained extensive follow-up photometry using the McDonald 2.1m Telescope and the ProEM frame-transfer camera. We obtained 5-30 s long exposures with the BG40 (9.9 h), i' (4.8 h), and z' (7.0 h) filters on UT 2015 June 9-12 and Aug 12-14.

2.3. Spectroscopy

We used the 8m Gemini North telescope with the Gemini Multi-Object Spectrograph (GMOS) to obtain medium resolution spectroscopy of J1529+2928 on 2015 July 7 and 10 as part of the program GN-2015A-DD-8. We obtained a sequence of 26×180 s exposures with the R831 grating and a $0.5''$ slit, providing wavelength coverage from 5500 Å to 7600 Å and a resolving power of 4396. We also obtained a sequence of 20×230 s exposures with the B1200 grating and a $0.5''$ slit, providing wavelength coverage from 3680 Å to 5140 Å and a resolving power of 3744. Each spectrum has a comparison lamp exposure taken within 10 min of the observation time. We measure radial velocities using the cross-correlation package RVSAO.

3. RESULTS

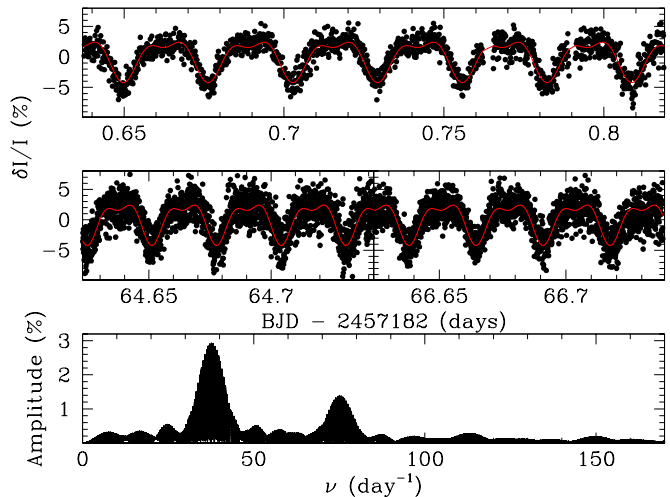


FIG. 1.— High speed BG40-filter photometry of J1529+2928 over 9.9 h (top and middle panels). The Fourier transform (bottom panel) shows a main peak at 37.74917(9) cycles d^{-1} and its first harmonic at 75.49834(21) cycles d^{-1} . The solid red line shows the predicted light curve based on these two frequencies.

3.1. The Period

Figure 1 shows the BG40-filter light curve of J1529+2928 obtained over 3 different nights at the McDonald Observatory 2.1m telescope. There are only two significant peaks in the Fourier Transform; the main peak is at 37.74917(9) cycles d^{-1} , 2288.792(6) s or 38.1 min, with a 2.95(4)% amplitude, and its first harmonic is detected at 75.49834(21) cycles d^{-1} . The light curve shows a strong dip in light that lasts about half the phase, a feature that looks like an eclipse. There is no evidence of any change in the ‘eclipse’ times over the 66 day baseline of these observations.

Our APO data with the BG40 filter span only 1.7 h, but the frequency and amplitude of the variations are consistent with the McDonald data within the errors. We detect 3.19(7)% photometric variations with a period of 2250(10) s. Similarly, we detect variations with periods of 2289(1) s and 2288(13) s in the i' and z' data, respectively. Since the BG40 filter data from the McDonald 2.1m telescope have the highest signal-to-noise ratio and the longest baseline, we adopt the best-fit period of 2288.792(6) s for J1529+2928 for the remainder of the paper.

3.2. No Stellar or Brown Dwarf Companions

Figure 2 shows trailed GMOS spectra of J1529+2928 for $H\gamma$, $H\beta$, and $H\alpha$. The latter was observed with the R831 grating over 85 min, and the former two lines were observed with the B1200 grating over 81 min. It is clear from this figure (especially given the narrow $H\alpha$ core) that there is no evidence of significant velocity variations in any of the Balmer lines. Forcing a fit at the photometric period of 2288.792 s yields a velocity semi-amplitude of $K = 3.6$ km s^{-1} . However, the F-test p-value is 0.94, which implies that this fit is consistent with scatter around the mean velocity. We perform 10,000 Monte-Carlo simulations assuming Gaussian errors and fixed period, and find that the average velocity semi-amplitude is $K = 4.9 \pm 2.7$ km s^{-1} .

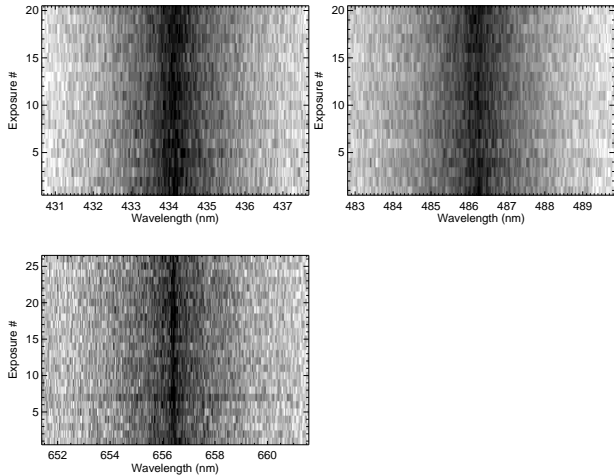


FIG. 2.— Gemini time-resolved spectroscopy of H γ (top left) and H β (top right) over 81 min, and that of H α (bottom left panel) over 85 min.

Figure 3 shows our 1D atmospheric model fits to the SDSS and Gemini spectra of J1529+2928. Fitting H β through H8, we derive $T_{\text{eff}} = 11450 \pm 200$ K and $\log g = 8.88 \pm 0.06$ from the SDSS spectrum and $T_{\text{eff}} = 11880 \pm 170$ K and $\log g = 8.78 \pm 0.04$ from the combined Gemini spectrum. Since Gemini observations have higher resolution and signal-to-noise ratio, we adopt the parameters from the GMOS data. Applying the 3D model atmosphere corrections (Tremblay et al. 2013) revise the temperature and surface gravity to $T_{\text{eff}} = 11580 \pm 170$ K and $\log g = 8.65 \pm 0.04$, respectively. These correspond to $M = 1.02 \pm 0.03 M_{\odot}$, $M_g = 12.8$ mag, $d = 83 \pm 3$ pc, $R = 0.0079 R_{\odot}$, $\log L/L_{\odot} = -3.0$, and an age of 1.3 Gyr.

Given the photometric period and the lack of significant velocity variations, the mass function is $f = 3 \pm 5 \times 10^{-7} M_{\odot}$. If the eclipses are due to a stellar or brown dwarf companion, the inclination would have to be almost 90° . For an edge-on orbit, the companion would be $0.007 M_{\odot}$, or $7 M_{\text{Jupiter}}$ at a separation of $0.38 R_{\odot}$. Hence, our radial velocity measurements rule out all stellar and brown dwarf companions around J1529+2928. In addition, all solid-body planetary objects are also ruled out as they would lead to very short transit durations of < 2 min.

J1529+2928 has a systemic velocity of $\gamma = 39 \pm 10$ km s^{-1} as measured from the SDSS spectrum. The expected gravitational redshift is 81.8 km s^{-1} . Hence, the true systemic velocity of J1529+2928 should be -42.8 ± 10 km s^{-1} .

4. DISCUSSION

4.1. Not Pulsations

Our 1D atmospheric parameters for J1529+2928 are within 1σ of the atmospheric parameters for the massive pulsating ZZ Ceti BPM 37093 (see §2.1 and Fig. 3). However, the photometric dips seen in J1529+2928 cannot be due to pulsations. All known DAVs have pulsation periods of ≤ 1200 s (e.g., Mukadam et al. 2006). BPM 37093 and GD 518, the two pulsators with $M \geq 1 M_{\odot}$, have pulsation periods of 512-635 s and 425-595 s, respectively (Metcalf et al. 2004; Hermes et al. 2013). On the

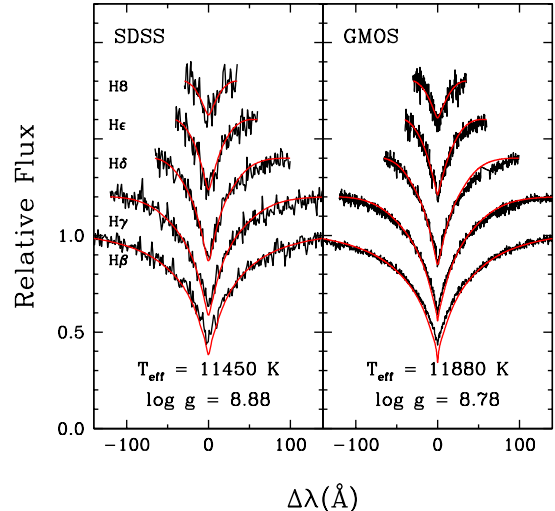


FIG. 3.— Model fits (red lines) to the Balmer line profiles of J1529+2928 from the SDSS (left panel) and Gemini (right panel) spectroscopy. Both fits show that H γ and H β are slightly filled in due to the flux contribution from a relatively cool starspot.

theoretical side, the buoyancy cutoff period for typical-mass WDs is ~ 1000 s, and almost certainly < 2000 s (Hansen et al. 1985). Hence, the 38 min period variability in J1529+2928 is not due to pulsations.

4.2. Not a Disintegrating Planet

The Roche Limit for Earth density objects around J1529+2928 is $1.4 R_{\odot}$ (Agol 2011). Hence, a putative 38 min period orbiting planet would be tidally disrupted. Such a planet would be falling apart after hundreds of orbits, yet Figure 1 clearly demonstrates that the photometric dips are constant over several weeks/months and that the hypothetical object is not appreciably changing. This implies that the ‘eclipses’ are not from a transiting object, but rather from a surface feature on the white dwarf itself.

Unlike the candidate disintegrating planet around WD 1145+017 (Vanderburg et al. 2015), there is no evidence of a debris disk around J1529+2928 based on the $3.6 \mu\text{m}$ photometry from the Wide-field Infrared Survey Explorer (WISE, Wright et al. 2010) mission. In addition, a relatively cool eclipsing planetary companion would lead to increasing eclipse depth as a function of wavelength. This is not seen in our photometric observations. Hence, the source of the photometric dips in J1529+2928 is not a disintegrating planet.

4.3. A Dark Spot on J1529+2928

Figure 4 shows the phased and binned BG40, i' , and z' light curves of J1529+2928. Here we used the best-fit period from the BG40 data, 2288.792 s, to phase the data in the other filters. The semi-amplitude of the photometric dips change from $2.95 \pm 0.04\%$ in the BG40 filter, to $2.30 \pm 0.11\%$ and $2.55 \pm 0.32\%$ in the i' and z' filter data, respectively. The z' data are relatively noisy and do not provide strong constraints on this system. However, the dips in the i' filter are significantly shallower than those in the BG40 filter. This clearly rules out a cool substellar companion around J1529+2928, and instead favors a

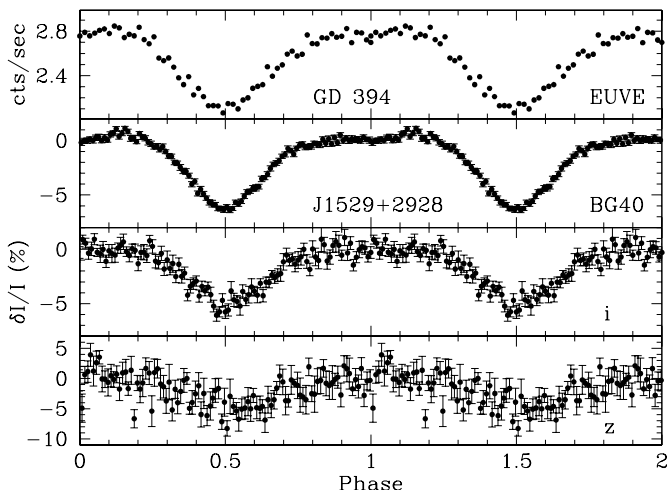


FIG. 4.— EUVE light curve of GD 394 (top panel, Dupuis et al. 2000), and the phased and binned light curves of J1529+2928 in the BG40, i' and z' filters. We used the best-fit period of 2288.792 s from the BG40 light curve to phase the i' and z' filter data.

starspot on the surface of the white dwarf. The spots on BOKS 53856 and WD 2359-434 were stable over several months (Holberg & Howell 2011; Gary et al. 2013), though the latter shows a slight decrease in amplitude over two years (B. Gary 2015, private communication). Hence, starspots can explain the stability of the photometric dips in our data spanning four months.

Figure 4 also shows the Extreme Ultraviolet Explorer (EUVE) data on GD 394 from Dupuis et al. (2000). The similarities between the GD 394 and J1529+2928 light curves are stunning. GD 394 is a relatively hot white dwarf with $T_{\text{eff}} = 39,440 \pm 350$ K and $\log g = 7.90 \pm 0.07$. The optical and ultraviolet spectra show strong Si features as well as a variety of trace elements including C, N, O, Al, and Fe. The Si abundance by number is $(\text{Si}/\text{H}) \sim 10^{-5}$. Dupuis et al. (2000) suggest that the 1.15 d period variability seen in the EUVE light curve of GD 394 is due to inhomogeneous abundance distribution of metals over the surface of the star. In their model, an almost circular spot with a higher heavy element abundance reduces the EUV emission over the spot region, causing 25% dips in brightness.

We do not have strong constraints on the metal abundances in J1529+2928 given the lack of high-resolution optical spectroscopy or ultraviolet data. However, there is a weak Ca K line in our GMOS spectrum at the same velocity as the Balmer lines. We measure an abundance of $\log(\text{Ca}/\text{H}) = -7.91$ from this line, but the spectrum is relatively noisy in this wavelength range and we take this measurement as an upper limit on the Ca abundance. Hence, metals are likely present in the atmosphere of J1529+2928 and are the likely cause of the periodic dips seen in its light curve. Since the opacity due to metals essentially decreases with increasing wavelength, a dark spot with a higher heavy element abundance would naturally explain the decrease in ‘eclipse’ depth in the BG40 and i -band data.

Both the SDSS and Gemini spectra (see Fig. 3) show that the observed line profiles are shallower than predicted by the best-fit model. The same is also true for

the $\text{H}\alpha$ line profiles. Assuming an inclination of 90° , a 10,000 K spot that covers 14% of the surface area of the white dwarf would explain the observed dips in both BG40 and i' filters. Due to the slight temperature difference between the spot and the white dwarf, such a spot also helps explain the observed $\text{H}\beta$ and $\text{H}\alpha$ line profiles. However, there are significant degeneracies in modelling of starspots due to unknown inclination, number of spots, spot latitude, and temperature (Dupuis et al. 2000), and further observations will be necessary to constrain the temperature of the spot region more accurately.

It is difficult to explain the presence of a spot on a white dwarf without invoking a magnetic field. Dupuis et al. (2000) constrain the magnetic field in GD 394 to $B < 12$ kG and they argue that such low field strengths may be enough to channel the accreted metals onto a spot if the accretion rate is low. Based on the lack of detection of Zeeman splitting of the narrow $\text{H}\alpha$ core, we derive an upper limit of $B < 70$ kG. Maxted et al. (2000), Wickramasinghe & Ferrario (2000), and Brinkworth et al. (2005) demonstrate that spotlike magnetic field enhancements extend to low field stars. They find a surface-wide 70 kG field and a localized 500 kG field to explain the 1.44 d period 2% peak-to-peak amplitude variations seen in WD 1953-011. Hence, a similar field structure could potentially explain the presence of spots on GD 394 and J1529+2928.

4.4. Implications for the Kepler/K2 missions and the LSST

GD 394 and J1529+2928 present excellent examples of apparently non-magnetic and isolated white dwarfs with spots. Both stars show significant dips in their light curves on hour-to-day timescales that are relatively easy to detect. The discovery of low-level (up to 0.2%) hour-to-day timescale variations in the Kepler data on apparently non-magnetic and isolated white dwarfs by Maoz et al. (2015) is therefore quite interesting. Maoz et al. (2015) present several scenarios to explain their observations, including but not limited to magnetic spots, hot spots from an interstellar medium accretion flow, transits by small planetary companions, or the reflection effect on a brown dwarf or giant planet companion.

Based on the detection of hour/day timescale photometric variations in strongly magnetic (e.g., RE J0317-853), weakly magnetic (e.g., WD 2359-434), and apparently non-magnetic (e.g., GD 394 and J1529+2928) white dwarfs, we suggest that many of the variable white dwarfs in the Kepler and K2 mission likely have starspots due to surface inhomogeneities and that the observed variability is a direct indicator of the rotation periods of these white dwarfs. The K2 mission will observe several hundred white dwarfs, and even with its decreased sensitivity compared to the original Kepler mission, it should still be able to find a relatively large number of variable white dwarfs and measure their rotation rates.

The LSST will image 13 million white dwarfs down to $r = 24.5$ mag and the design goals include photometric repeatability of 5 mma at the bright end. The photometric precision of each visit will be worse at fainter magnitudes, e.g. 1% at $r = 21$ mag and 2% at $r = 22$ mag (Ivezic et al. 2008). Only one of the 15 white dwarfs (6.7%) observed by the Kepler mission, BOKS 53856, dis-

plays photometric variations larger than a few per cent. Eleven out of the 74 (15%) white dwarfs within 20 pc of the Sun are magnetic with $B \geq 100$ kG (Kawka et al. 2007). In addition, Brinkworth et al. (2013) find 1-2% variability in 2/3 of their $B \geq 100$ kG magnetic white dwarf sample, implying an overall variability fraction of 10%. Sion et al. (2014) find the fraction of magnetic white dwarfs in the 25 pc local sample to be $\geq 8\%$, but Liebert et al. (2003) demonstrate that the fraction could be substantially higher than 10% for $B > 10$ kG. Hence, with a 1% precision at $r = 21$ mag, the LSST may find $\sim 10^5$ white dwarfs that show variations on hour/day timescales due to the presence of magnetic fields.

5. CONCLUSIONS

We present the discovery of 38 min period eclipse-like events in the light curve of the massive white dwarf J1529+2928. We rule out stellar and brown dwarf companions based on the lack of significant radial velocity variations, and demonstrate that the dips in the light curve are likely caused by a dark spot that comes into view every 38 min due to the rotation of the white dwarf.

The presence of a spot on J1529+2928 almost certainly requires a magnetic field. However, there is no evidence of Zeeman splitting of the Balmer lines in our optical spectroscopy, constraining the magnetic field strength to $B < 70$ kG. Follow-up high resolution optical spectroscopy or spectropolarimetry would be useful to search for a magnetic field and constrain its strength.

A weak Ca K line is present in our spectrum, though follow-up UV spectroscopy would be useful to confirm the presence of metals and constrain their abundances in J1529+2928. Dupuis et al. (2000) demonstrate that accreted metals concentrated on a spot by a magnetic field would lead to an enhanced opacity source when the spot is in view, and this could explain the observed EUV light curve of GD 394. The same model would also explain the differing ‘eclipse’ depths in J1529+2928 in different filters. Dupuis et al. (2000) predict that the UV and optical light curves should be in antiphase due to the flux redistribution effect. Follow-up concurrent UV and optical photometry observations can test this hypothesis.

Finally, based on the discovery of significant photometric variations in apparently non-magnetic white dwarfs like GD 394 and J1529+2928, we discuss the high incidence of photometric variability observed in the Kepler and K2 missions. We argue that the source of the variability is most likely related to the presence of weak magnetic fields, and that current and future transient surveys like the LSST should find a significant number of white dwarfs that display hour-to-day timescale photometric variations.

We gratefully acknowledge the support of the NSF and NASA under grants AST-1312678, AST-1312983, and NNX14AF65G.

Facilities: Gemini (GMOS), APO 3.5m (Agile), McDonald 2.1m (ProEM)

REFERENCES

- Agol, E. 2011, *ApJ*, 731, L31
 Aznar Cuadrado, R., Jordan, S., Napiwotzki, R., et al. 2004, *A&A*, 423, 1081
 Barstow, M. A., Jordan, S., O’Donoghue, D., et al. 1995, *MNRAS*, 277, 971
 Brinkworth, C. S., Marsh, T. R., Morales-Rueda, L., et al. 2005, *MNRAS*, 357, 333
 Brinkworth, C. S., Burleigh, M. R., Lawrie, K., Marsh, T. R., & Knigge, C. 2013, *ApJ*, 773, 47
 Dupuis, J., Chayer, P., Vennes, S., Christian, D. J., & Kruk, J. W. 2000, *ApJ*, 537, 977
 Ferrario, L., Vennes, S., Wickramasinghe, D. T., Bailey, J. A., & Christian, D. J. 1997, *MNRAS*, 292, 205
 Gary, B. L., Tan, T. G., Curtis, I., Tristram, P. J., & Fukui, A. 2013, Society for Astronomical Sciences Annual Symposium, 32, 71
 Gianninas, A., Bergeron, P., & Ruiz, M. T. 2011, *ApJ*, 743, 138
 Hallakoun, N., Maoz, D., Kilic, M., et al. 2015, *MNRAS*, submitted, arXiv:1507.06311
 Hansen, C. J., Winget, D. E., & Kawaler, S. D. 1985, *ApJ*, 297, 544
 Hermes, J. J., Kepler, S. O., Castanheira, B. G., et al. 2013, *ApJ*, 771, L2
 Hermes, J. J., Brown, W. R., Kilic, M., et al. 2014, *ApJ*, 792, 39
 Holberg, J. B., & Howell, S. B. 2011, *AJ*, 142, 62
 Ivezić, Z., Tyson, J. A., Abel, B., et al. 2008, arXiv:0805.2366
 Kawka, A., Vennes, S., Schmidt, G. D., Wickramasinghe, D. T., & Koch, R. 2007, *ApJ*, 654, 499
 Kilic, M., Brown, W. R., Kenyon, S. J., et al. 2011, *MNRAS*, 413, L101
 Kleinman, S. J., Kepler, S. O., Koester, D., et al. 2013, *ApJS*, 204, 5
 Landolt, A. U. 1968, *ApJ*, 153, 151
 Liebert, J., Bergeron, P., & Holberg, J. B. 2003, *AJ*, 125, 348
 Loeb, A., & Gaudi, B. S. 2003, *ApJ*, 588, L117
 Maoz, D., Mazeh, T., & McQuillan, A. 2015, *MNRAS*, 447, 1749
 Maxted, P. F. L., Ferrario, L., Marsh, T. R., & Wickramasinghe, D. T. 2000, *MNRAS*, 315, L41
 Metcalfe, T. S., Montgomery, M. H., & Kanaan, A. 2004, *ApJ*, 605, L133
 Mukadam, A. S., Mullally, F., Nather, R. E., et al. 2004, *ApJ*, 607, 982
 Mukadam, A. S., Montgomery, M. H., Winget, D. E., Kepler, S. O., & Clemens, J. C. 2006, *ApJ*, 640, 956
 Parsons, S. G., Gänsicke, B. T., Marsh, T. R., et al. 2013, *MNRAS*, 429, 256
 Shporer, A., Kaplan, D. L., Steinfadt, J. D. R., et al. 2010, *ApJ*, 725, L200
 Sion, E. M., Holberg, J. B., Oswalt, T. D., et al. 2014, *AJ*, 147, 129
 Tremblay, P.-E., Ludwig, H.-G., Steffen, M., & Freytag, B. 2013, *A&A*, 559, A104
 Vanderburg, A., Johnson, J. A., Rappaport, S., et al. 2015, *Nature*, in press
 Wickramasinghe, D. T., & Ferrario, L. 2000, *PASP*, 112, 873
 Wright, E. L., Eisenhardt, P. R. M., Mainzer, A. K., et al. 2010, *AJ*, 140, 1868
 Zucker, S., Mazeh, T., & Alexander, T. 2007, *ApJ*, 670, 1326